Progress In Electromagnetics Research Letters, Vol. 99, 35–43, 2021

A Low-Profile Half-Mode Substrate Integrated Waveguide Filtering Antenna with High Frequency Selectivity

Hai-Yan Wang, Gang Zhao*, Rui-Yang Li, and Yong-Chang Jiao

Abstract—A low-profile half-mode substrate integrated waveguide (HMSIW) filtering antenna with high frequency selectivity is proposed in this letter. The proposed antenna with a height of $0.014\lambda_0$ (λ_0 is the free-space wavelength) consists of a slot-loaded HMSIW cavity, two parasitic patches, and five shorting pins. An upper-edge radiation null is generated by the interaction between the HMSIW cavity and parasitic patches. A rectangular slot etched on the HMSIW cavity is adopted to generate another null to improve the filtering performances at the upper stopband. Besides, the radiation in the lower stopband is suppressed by two nulls which emerge due to placing shorting pins under two parasitic patches. Thus, four radiation nulls can be obtained to enhance the frequency selectivity. The measured results illustrate that the proposed antenna provides an impedance bandwidth of 4.3% ranging from 2.74 to 2.86 GHz and a peak gain of 6.76 dBi during the operating frequency band. Moreover, four radiation nulls appear at 2.34, 2.56, 3, and 3.24 GHz in the lower and upper stopbands.

1. INTRODUCTION

With the rapid development of wireless communication technology, the combination of different components to meet multi-function and miniaturization requirements has aroused great interest. Therefore, the integration of filter and antenna has been widely researched owing to its superior performance. Conventionally, filtering antennas are realized by cascading the individually designed filter and antenna with each other or designing the antenna as the last-order resonator of the filter. However, the multiple resonators occupy a lot of space and add the complexity of the system. In recent years, the integration design of antennas with filters, which introduces radiation nulls on edges of the operating band, becomes an effective method to obtain good frequency selectivity with much fewer resonators.

Various antennas have been developed to obtain excellent filtering performances, including Yagi Uda antennas [1], dielectric resonator antennas [2–6], microstrip patch antennas [7–11], and substrate integrated waveguide (SIW) antennas. Due to the virtues of low loss and high radiation efficiency, SIW has been widely applied to design excellent filtering antennas [12–25]. By vertically stacking the resonators, multilayered 3-D configurations are designed in [14–19]. In [14], two radiation nulls were produced by combining a slot-backed substrate integrated cavity and stacked patches. A second-order filtering antenna has been realized by using a SIW bandpass filtering circuit together with a printed antipodal linearly tapered slot antenna. The electric and magnetic mixed-coupling structures generate adjustable transmission zeros [15]. In the work of [17], two non-radiating modes (i.e., TE_{010} mode and TE_{110} mode) are utilized to generate radiation nulls. Although these multilayered configurations make the frequency selectivity improved, they bring about high profile and fabrication complexities. Given this, the filtering antenna using a single-layered SIW cavity was proposed in [20–25]. Conventional

Received 12 May 2021, Accepted 14 July 2021, Scheduled 19 July 2021
* Corresponding author: Gang Zhao (gangzhao@mail.xidian.edu.cn).
The authors are with the National Key Laboratory of Antennas and Microwave Technology, Xidian University, Xi'an 710071, P. R. China.

SIW cavities were employed to enhance the selectivity of channel responses in [22]. In [25], a SIW filtering antenna with parasitic patches was designed to improve impedance bandwidth and filtering performances. However, most of the previous works can only acquire good frequency selectivity at single-side stopband, and the design for achieving good frequency selectivity on both edges of the passband is of great research value.

To solve the above-mentioned problems, a low-profile half-mode substrate integrated waveguide (HMSIW) filtering antenna with high selectivity is proposed. The antenna is composed of a slot-loaded HMSIW cavity, two rectangular patches, and five shorting pins. To retain the merits of SIW but the size is half reduced, the HMSIW is selected to design the filtering antenna [26]. Two patches are adopted as the parasitic elements, which not only generates a good filtering response at the upper stopband but also improves its impedance bandwidth. Moreover, an additional slot and shorting pins are used to introduce another radiation null, hence realizing better filtering performances. To verify the validity of the proposed design, a prototype is fabricated and measured. The measured results demonstrate that both good radiation and filtering performances are achieved.

2. ANTENNA DESIGN

2.1. Antenna Configuration

The configuration of the proposed filtering antenna is shown in Fig. 1, and the Taconic TLY-5 with $\varepsilon_r = 2.2$ and $h = 1.5\,\text{mm}$ is chosen as substrate. The proposed antenna is composed of an HMSIW cavity, two parasitic patches, and five shorting pins. Shorting pins with diameter p are placed along the middle line of the patches to obtain a quasi-symmetrical radiation pattern. As shown in Fig. 2,

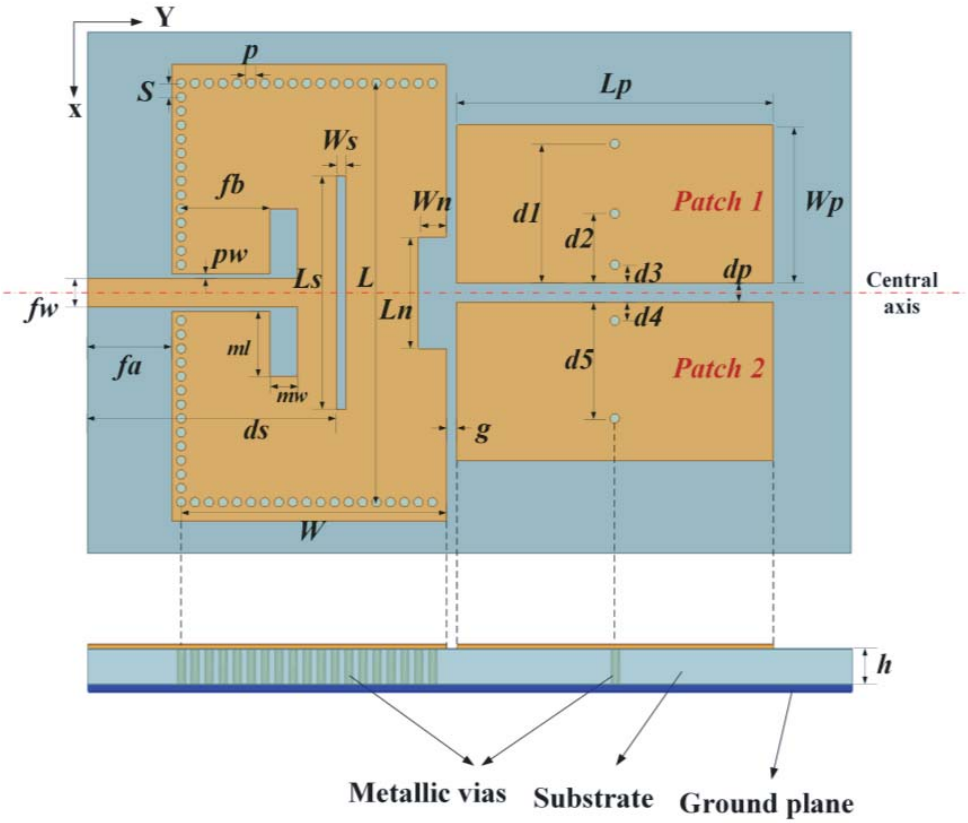

Figure 1. Geometry of the proposed antenna and its optimized design parameters in millimeters. $p = 1$, $s = 1.5$, $L = 46$, $W = 28$, $Lp = 34$, $Wp = 17$, $fa = 9$, $fb = 12$, $fw = 3$, $pw = 0.5$, $ml = 7.5$, $mw = 3$, $Ls = 25$, $Ws = 1$, $ds = 26.7$, $Ln = 12$, $Wn = 3$, $d1 = 16$, $d2 = 8.5$, $d3 = 3$, $d4 = 3$, $d5 = 13.5$, $g = 1.1$ and $dp = 2$.

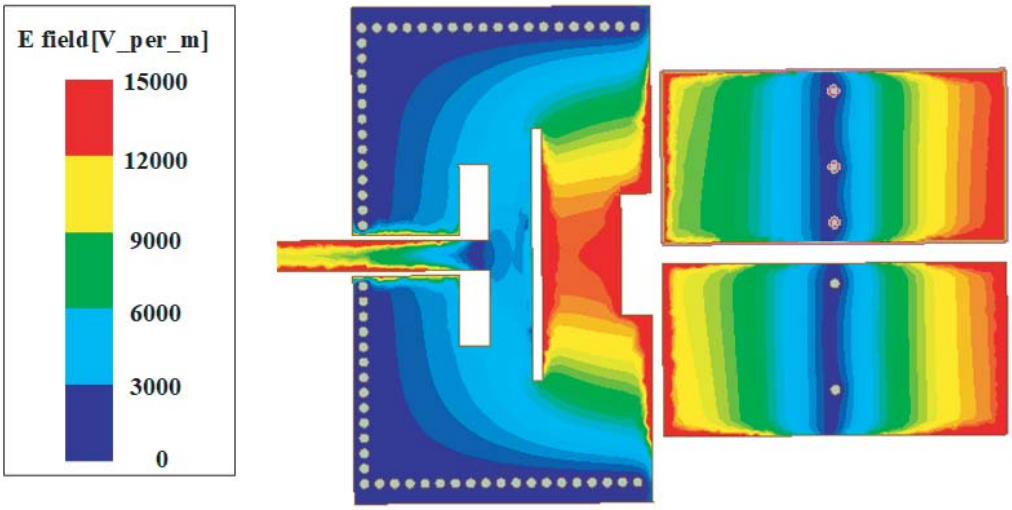

Figure 2. Electric field magnitude distributions of the cavity and the parasitic patch at the central operating frequency.

the HMSIW cavity and patches are designed to work in the TE_{110} mode and TM_{01} mode respectively at the center frequency. The HMSIW cavity is designed with a dielectric constant of $\varepsilon_r = 2.2$ and dimensions of $L \times W \times h$, operating at 2.8 GHz with TE_{110} mode. The initial dimensions of HMSIW can be predicted using the following equation [27]:

$$f_{mn0} = \frac{\mathrm{c}}{2\pi\sqrt{u_r\varepsilon_r}}k_0 \tag{1}$$

$$k_0^2 = k_x^2 + k_y^2 \tag{2}$$

where c is the free-space velocity of light; k_0 is the free space wavenumber of TE_{110} mode; k_x and k_y are the wave numbers in x and y directions, respectively. The wave numbers can be calculated by

$$k_x = \frac{\pi}{L}, \quad k_y = \frac{\pi}{2W}, \quad k_0 = \frac{2\pi}{\lambda_0} \tag{3}$$

Meanwhile, rectangular patches that are symmetric concerning the central axis are well excited by the HMSIW cavity. Initial dimensions of patches can be estimated by [28]:

$$f_{01} = \frac{c}{2L_p\sqrt{\varepsilon_r}} \tag{4}$$

The grounded coplanar waveguide (GCPW) is employed as the feeding structure which directly excites the HMSIW cavity. A notch with a size of $Ls \times Ws$ is cut along the edge of the HMSIW cavity to improve its impedance match. The filtering antenna is simulated and optimized by Ansys HFSS software.

2.2. Operating Principle

As depicted in Figs. 3(a) and (b), structure I and structure II with the same dimensions are introduced to explicate the filtering characteristics of the proposed antenna. Structure I includes an HMSIW cavity and parasitic patches. Based on this structure, structure II is formed by etching a rectangular slot with the length of $1/4\lambda_0$ on the HMSIW cavity. The slot loaded on HMSIW blocks the current flowing to the radiating side, and the energy is mainly concentrated near the slot. When the length of the slot is selected reasonably, the surface current is equal in magnitude and opposite in direction along the long edges of the slot [29]. The simulated broadside gains are presented in Fig. 3(d). It can be observed that structure I generates a radiation null at the upper stopband while structure II generates another

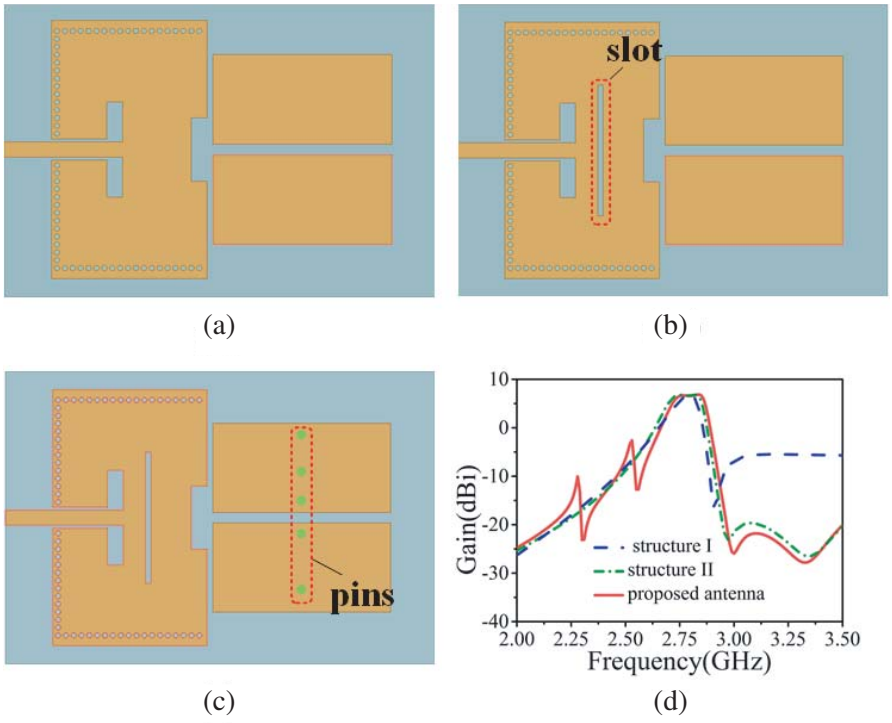

Figure 3. Three different types of structures. (a) Structure I. (b) Structure II. (c) Proposed structure. (d) Simulated gains of three antenna structures.

one independently. However, no radiation nulls have been obtained at the lower edge of the operating band. Therefore, five shorting pins are adopted to introduce two lower-edge radiation nulls in Fig. 3(c). Consequently, four radiation nulls are generated on both edges of the passband, thus bring out good filtering performance.

For explicating the operation mechanism of four radiation nulls clearly, the current distributions on the parasitic patches and HMSIW cavity at center and radiation nulls frequencies are shown in Fig. 4. In Fig. 4(a), there are opposite currents on the left and right sides of patch 2 resulting in far-field radiation cancellation in the broadside direction, which generates a radiation null at 2.32 GHz. Fig. 4(b) indicates that the current distribution on patch 1 resembles the one on patch 2 in Fig. 4(a), which introduces another radiation null at 2.55 GHz. Loading more shorting pins on patches means that the inductance increases; therefore, two different radiation nulls are generated at the lower stopband. It can be observed in Fig. 4(c) that currents on surfaces of the HMSIW cavity and patches are out-of-phase along the central axis at 3 GHz, which would offset each other's contributions on the broadside radiation. As indicated in Fig. 4(d), a slot etched on the HMSIW cavity generates a radiation null at 3.34 GHz due to the radiation suppression caused by opposite currents along the slot. Two patches and the HMSIW cavity can radiate effectively, as exhibited in Fig. 4(e).

2.3. Parametric Study

Figure 5 indicates the effects of ds, g, dp, and N on the reflection coefficient and gain of the proposed antenna. For the sake of convenience, null1, null2, null3, and null4 are used to represent the radiation nulls at 2.32, 2.55, 3, and 3.34 GHz, respectively. It is observed clearly in Fig. 5(a) that with the decrease of ds, the null4 moves down while the suppression level increases. The location of the null3 can be controlled by altering g, as shown in Fig. 5(b). Additionally, as g increases, the suppression level decreases at the upper stopband but increases at the lower stopband. It is presented in Fig. 5(c) that dp has a great influence on the lower-edge radiation nulls. Especially, when Patch 1 and Patch 2 are combined into a single patch ($dp = 0$ mm), there is only one lower-edge radiation null left. When

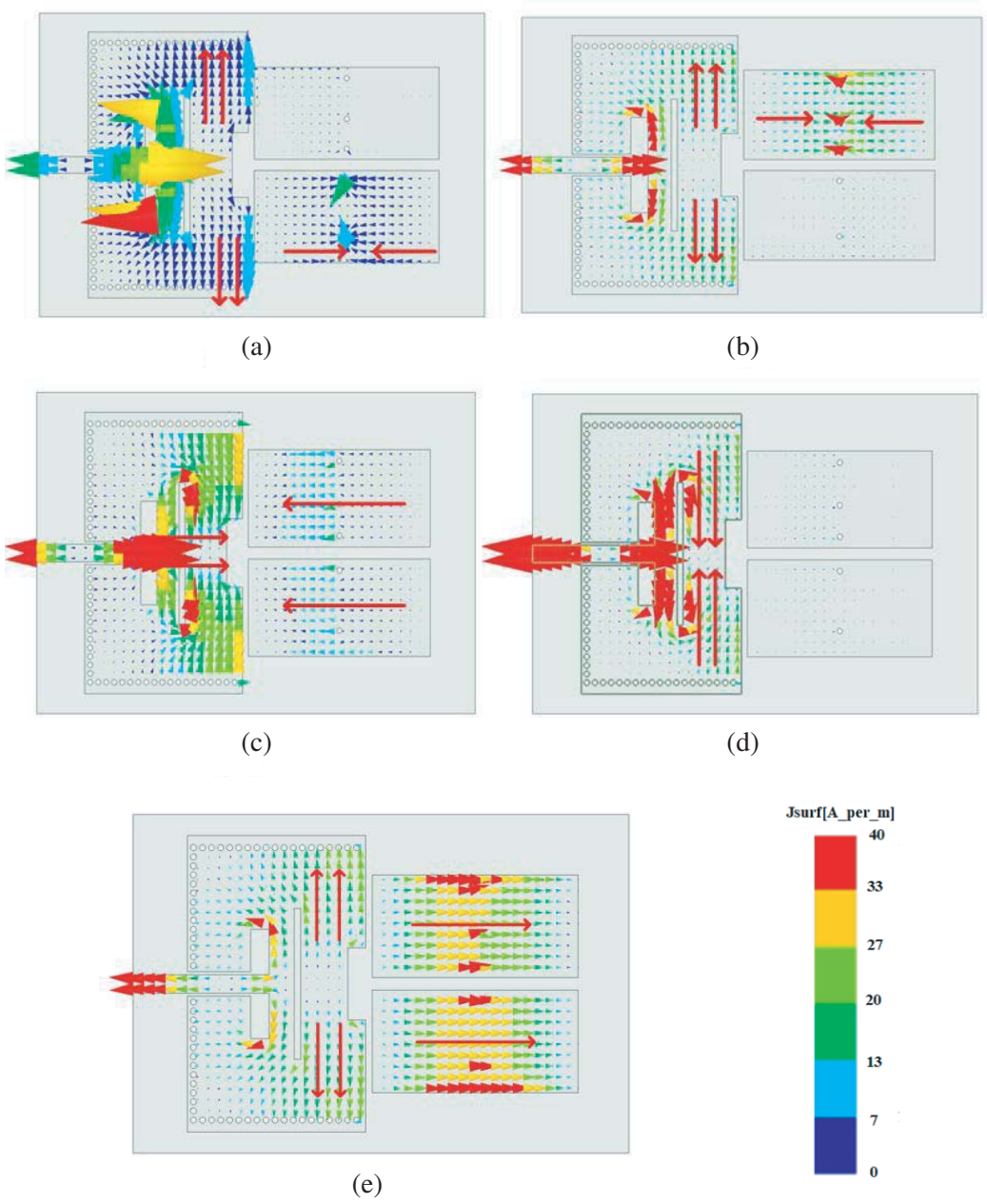

Figure 4. Current distributions on the surfaces of the HMSIW cavity and parasitic patches at (a) 2.32 GHz, (b) 2.55 GHz, (c) 3 GHz, (d) 3.34 GHz, (e) 2.8 GHz.

the number of shorting pins N added on Patch 1 increases, the null2 moves up, and the suppression level decreases in the meantime as indicated in Fig. 5(d). This is because loading more shorting pins makes the resonance stronger and leads to the gain increased at the corresponding frequency. Taking bandwidth and band-edge roll-off rates into consideration, the physical parameters $ds = 26.7$ mm, $g = 1$ mm, $dp = 2$ mm, and $N = 3$ are selected. The height of the substrate, h, also has a great influence on the proposed antenna performance. Thus, it should be optimized reasonably.

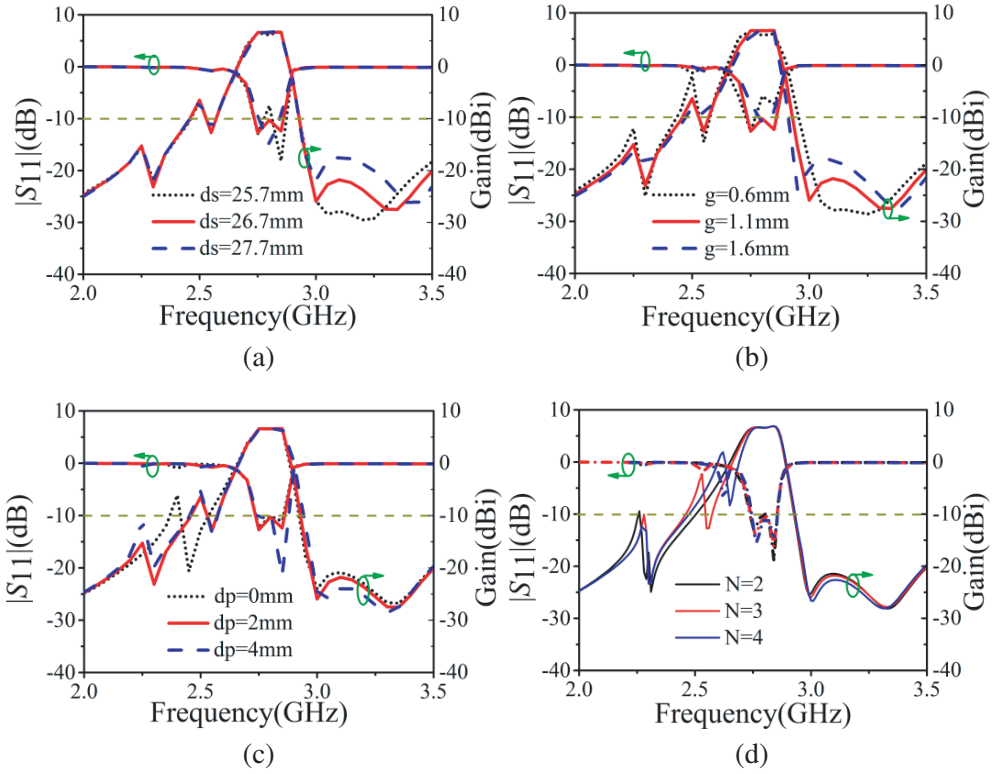

Figure 5. Simulated performances variation with different parameters. (a) *ds*. (b) *g*. (c) *dp*. (d) *N* (the number of pins loaded on patch 1).

3. RESULTS AND DISCUSSION

To validate the design method, a prototype is fabricated and measured, and the antenna photograph is shown in Fig. 6(a). The reflection coefficient is measured with an Anritsu MS46322A vector network analyzer, while the radiation patterns and gains are measured in a microwave anechoic chamber with a far-field measurement method. The measured and simulated reflection coefficients and realized gains are presented in Fig. 6(b). The simulated operating band is from 2.74 to 2.85 GHz while the measured results demonstrate that the 10 dB impedance bandwidth is about 4.3% ranging from 2.74 to 2.86 GHz. During the operating band, the peak gain reaches 6.76 dBi, and the total efficiency calculated based on simulated results is at least 91%. Four radiation nulls at 2.34, 2.56, 3, and 3.24 GHz are achieved on both edges of the operating band. The lower and upper band-edge roll-off rates are 175 and 183 dB/GHz, respectively. Especially, the proposed antenna has better filtering performance at the upper stopband since the upper band rejection is more than 22 dB while the lower one is more than 9 dB. Figs. 6(c) and (d) show the radiation patterns in E/H-plane at 2.8 GHz. It can be observed that radiation patterns almost keep symmetrical in both planes. Due to the asymmetry of the whole structure, the E-plane pattern is slightly inclined. Besides, the measured cross-polarization levels are better than 20 dB in E/H-plane.

The performance comparison is provided in Table 1 to show the merit of our proposed filtering antenna. Compared with the multilayer SIW structures designed in [12, 14, 17–19], the proposed single-layer antenna in this work has the advantage of low profile and more radiation nulls. Besides, the proposed antenna has a smaller transverse size and better frequency selectivity than the designs in [12, 14, 17]. The proposed antenna achieves higher efficiency during operation band and wider bandwidth than the design in [18, 19]. Compared with the filtering antenna designed with a single-layer SIW structure in [25], the proposed antenna shows more radiation nulls and better frequency selectivity in general.

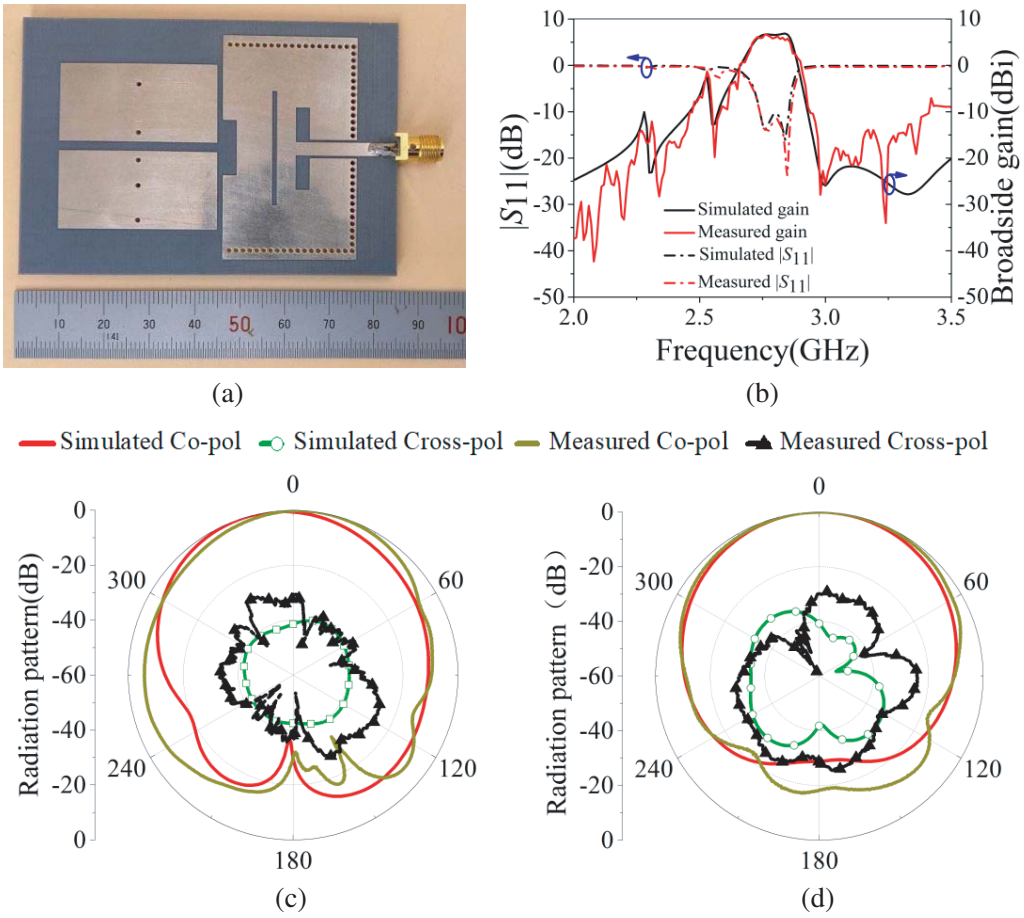

Figure 6. (a) Photograph of the proposed antenna. (b) Simulated and measured reflection coefficients and gains of the proposed antenna. (c) Simulated and measured radiation patterns at 2.8 GHz in E-plane. (d) Simulated and measured radiation patterns at 2.8 GHz in H-plane.

Table 1. Performance summary of the proposed and state-of-art designs.

Ref.	Transverse Size (λg^2)	Height (λ_0)	BW (%)	η (%)	NRNs	Lower/Upper Selectivity (dB/GHz)
[12]	2.24	0.07	1.6	N.A.	2	26/57
[14]	3.10	0.13	9.1	87	2	48/165
[17]	3.8	0.13	8.7	N.A.	2	38/58
[18]	0.85	0.07	1.4	79.3	2	210/108
[19]	0.81	0.12	3.0	58.9	0	63/28
[25]	0.15	0.015	5.1	N.A.	2	68/233
This work	0.18	0.014	4.2	91	4	175/183

BW: 10 dB impedance bandwidth. NRNs: The number of radiation nulls. Lower/Upper Selectivity is calculated as $|\alpha_{\max} - \alpha_{\min}|/|f_z - f_c|$, where $\alpha_{\max}$ is the attenuation of the first out-of-band radiation null or 20 dB attenuation if no radiation null and $\alpha_{\min}$ is the 3 dB attenuation; f_z and f_c are their corresponding frequency.

4. CONCLUSIONS

In this letter, A low-profile HMSIW filtering antenna with high frequency selectivity is proposed. A slot-loaded HMSIW cavity and two parasitic patches with shorting pins are adopted to generate four radiation nulls. The interaction between the HMSIW cavity and parasitic patches generates a filtering response at the upper stopband edge. Meanwhile, an additional slot and shorting pins are adopted to introduce another three radiation nulls to realize better filtering performances. The measured results indicate that the proposed antenna has excellent frequency selectivity on both edges of the passband with roll-off rates of 175 and 183 dB/GHz.

REFERENCES

1. Shi, J., X. Wu, and Z. N. Chen, "A compact differential filtering quasi-Yagi antenna with high frequency selectivity and low cross-polarization levels," *IEEE Antennas Wireless Propag. Lett.*, Vol. 14, 1573–1576, 2015.
2. Hu, P. F., Y. M. Pan, and X. Y. Zhang, "Broadband filtering dielectric resonator antenna with wide stopband," *IEEE Trans. Antennas Propag.*, Vol. 65, No. 4, 2079–2084, Apr. 2017.
3. Chu, H., H. Hong, and X. H. Zhu, "Implementation of synthetic material in dielectric resonator-based filtering antennas," *IEEE Trans. Antennas Propag.*, Vol. 66, No. 7, 3690–3695, Jul. 2018.
4. Tang, H., C. W. Tong, and J. X. Chen, "Differential dual-polarized filtering dielectric resonator antenna," *IEEE Trans. Antennas Propag.*, Vol. 66, No. 8, 4298–4302, Aug. 2018.
5. Hu, P. F., Y. M. Pan, and X. Y. Zhang, "A compact quasi-isotropic dielectric resonator antenna with filtering response," *IEEE Trans. Antennas Propag.*, Vol. 67, No. 2, 1294–1299, Feb. 2019.
6. Gao, Y., Y. C. Jiao, and Z. B. Weng, "A filtering dielectric resonator antenna with high band-edge selectivity," *Progress In Electromagnetics Research M*, Vol. 89, 63–71, 2020.
7. Wang, Y., Y. L. Chen, and J. F. Qian, "A dual-mode resonator-fed gap coupled filtering antenna with improved selectivity and bandwidth," *Progress In Electromagnetics Research Letters*, Vol. 87, 137–143, 2019.
8. Liu, G., Y. M. Pan, and X. Y. Zhan, "Compact filtering patch antenna arrays for marine communications," *IEEE Trans. Antennas Propag.*, Vol. 69, No. 10, 11408–11418, Oct. 2020.
9. Hu, H. T., F. C. Chen, and Q. X. Chu, "Novel broadband filtering slotline antennas excited by multimode resonators," *IEEE Antennas Wireless Propag. Lett.*, Vol. 16, 489–492, 2017.
10. Mao, C. X., S. Gao, and Y. Wang, "Dual-band patch antenna with filtering performance and harmonic suppression," *IEEE Trans. Antennas Propag.*, Vol. 64, No. 9, 4074–4077, Sep. 2016.
11. Hsieh, C. Y., C. H. Wu, and T. G. Ma, "A compact dual-band filtering patch antenna using step impedance resonators," *IEEE Antennas Wireless Propag. Lett.*, Vol. 14, 1056–1059, 2015.
12. Chu, H., C. Jin, and J. X. Chen, "A 3-D millimeter-wave filtering antenna with high selectivity and low cross-polarization," *IEEE Trans. Antennas Propag.*, Vol. 63, No. 5, 2375–2380, May 2015.
13. Liu, Q., D. F. Zhou, and J. Shi, "High-selective triple-mode SIW bandpass filter using higher-order resonant modes," *Electronics Letters*, Vol. 56, No. 1, 37–39, Jan. 2020.
14. Liu, X., X. F. Zhang, and K. Xu, "A filtering antenna with high frequency selectivity using stacked dual-slotted substrate integrated cavities," *IEEE Antennas Wireless Propag. Lett.*, Vol. 19, No. 8, 1311–1315, Aug. 2020.
15. Hua, C. Z., X. Y. Jin, and M. Liu, "Design of compact vertically stacked SIW end-fire filtering antennas with transmission zeros," *Progress In Electromagnetics Research Letters*, Vol. 87, 67–73, 2019.
16. Fan, C., B. Wu, and Y. L. Wang, "High-gain SIW filtering antenna with low H-plane cross polarization and controllable radiation nulls," *IEEE Trans. Antennas Propag.*, Vol. 69, No. 4, 2336–2340, Apr. 2021.
17. Xu, K., J. Shi, and X. M. Qing, "A substrate integrated cavity backed filtering slot antenna stacked with a patch for frequency selectivity enhancement," *IEEE Antennas Wireless Propag. Lett.*, Vol. 17, No. 10, 1910–1914, Oct. 2018.

18. Niu, B. J. and J. H. Tan, "Dual-layer SIW cavity filtering antenna with a controllable radiation band and two radiation nulls," *Electronics Letters*, Vol. 55, No. 13, 723–724, Jun. 2019.
19. Yusuf, Y., H. T. Cheng, and X. Gong, "A seamless integration of 3-D vertical filters with highly efficient slot antennas," *IEEE Trans. Antennas Propag.*, Vol. 59, No. 11, 4016–4022, Nov. 2011.
20. Liu, Q., D. F. Zhou, and D. L. Lv, "Realisation of compact quasi-elliptic bandpass filters based on coupled eighth-mode SIW cavities," *IET Microw. Antennas Propag.*, Vol. 13, No. 13, 2256–2263, Jul. 2019.
21. Deng, H. W., L. Sun, and Y. F. Xue, "High selectivity and common-mode suppression balanced bandpass filter with TM dual-mode SIW cavity," *IET Microw. Antennas Propag.*, Vol. 13, No. 12, 2129–2133, Jul. 2019.
22. Dhwaj, K., X. Q. Li, and L. J. Jiang, "Low-profile diplexing filter/antenna based on common radiating cavity with quasi-elliptic response," *IEEE Antennas Wireless Propag. Lett.*, Vol. 17, No. 10, 1783–1787, Oct. 2018.
23. Liu, Q. W., L. Zhu, and J. P. Wang, "A wideband patch and SIW cavity hybrid antenna with filtering response," *IEEE Antennas Wireless Propag. Lett.*, Vol. 19, No. 5, 836–840, May 2020.
24. Li, P. K., C. J. You, and H. F. Yu, "Codesigned high-efficiency single-layered substrate integrated waveguide filtering antenna with a controllable radiation null," *IEEE Antennas Wireless Propag. Lett.*, Vol. 17, No. 2, 295–298, Feb. 2018.
25. Hu, K. Z., M. C. Tang, and D. J. Li, "Design of compact, single-layered substrate integrated waveguide filtenna with parasitic patch," *IEEE Trans. Antennas Propag.*, Vol. 68, No. 2, 1134–1139, Feb. 2020.
26. Hong, W., et al. (Keynote Talk), "Half mode substrate integrated waveguide: A new guided wave structure for microwave and millimeter wave application," *Joint 31st Int. Conf. on Infrared and Millimeter Waves and 14th Int. Conf. on Terahertz Electronics*, Shanghai, Sept. 18–22, 2006.
27. Zhou, K., C.-X. Zhou, and W. Wu, "Resonance characteristics of substrate-integrated rectangular cavity and their applications to dualband and wide-stopband bandpass filters design," *IEEE Trans. Microw Theory Techn.*, Vol. 65, No. 5, 1511–1524, May 2017.
28. Balanis, C. A., *Antenna Theory: Analysis and Design*, 3rd Edition, Wiley, New York, NY, USA, 2005.
29. Li, L., D. Pang, and Y. B. Feng, "A low-profile third-order half-mode SIW filtering antenna with low H-plane cross polarization and good sideband suppression," *IEEE Antennas Wireless Propag. Lett.*, Vol. 18, 2503–2507, 2019.